

PINK SPINEL IN APOLLO IMPACT MELT ROCK 68815: IMPLICATIONS FOR MG-SUITE MAGMATISM. A. C. Stadermann¹, J. J. Barnes¹, T. M. Erickson², Z. D. Michels³, and T. C. Prissel², ¹Lunar and Planetary Laboratory, University of Arizona, 1629 E University Blvd, Tucson, AZ 85721 (stadermann@email.arizona.edu), ²Jacobs – NASA Johnson Space Center, 2101 E NASA Pkwy, Houston, TX 77058, ³Department of Geosciences, University of Arizona, 1040 E. 4th Street, Tucson, AZ 85721.

Introduction: Magnesian rocks from the lunar highlands are collectively termed the Mg-suite. Characterized by high (>60) Mg# (molar $100 \times \text{Mg}/[\text{Mg}+\text{Fe}]$) in mafic phases and calcic plagioclase, these rocks are plutonic to hypabyssal in origin, and include a range of bulk mineralogies such as troctolites, dunites, norites, gabbronrites, and spinel troctolites [1]. These Mg-suite lithologies have distinct trace element concentrations and ratios that differentiate them from other lunar rock types. These rocks are ancient, generally dated to between 4.5 and 4.1 Ga, although it is unknown if this represents the full range of Mg-suite ages [1–2].

Among the Mg-suite lithologies, the spinel troctolites are relatively rare, to date only found in polymict breccias [3]. Spinel troctolites, as their name suggests, consist of calcic plagioclase and forsteritic olivine, with minor amounts of spinel (MgAl_2O_4), \pm pyroxene and cordierite [1,4]. This form of spinel is often called ‘pink’ spinel because of its appearance in thin section under plane polarized light (PPL; Fig. 1), due to minor amounts of Cr. Spinel troctolites are generally plutonic or hypabyssal in origin (subsequently exhumed and incorporated into polymict breccias), or formed through impact processes (e.g., crystalline impact melt) [5]. A spinel-rich lithology has also been found in the Moscovien region of the Moon via the Moon Mineralogy Mapper (M^3) and lacks other mafic phases [6]. Finally, while the Mg-suite sampled thus far consists of plutonic (or hypabyssal) rocks, the question remains if such magmas could have erupted on the surface of the Moon [7]. These magmas have much lower density than mare basalts, but little sample or remote sensing evidence has been found to support the idea that extrusive Mg-suite volcanism occurred [7].

Here, we present a coordinated microanalytical study of spinel-bearing lithic and mineral clasts found in Apollo sample 68815. These data will be used to understand their petrogenesis (magmatic or impact) and modification histories, and to shed light on the existence of volcanic Mg-suite rocks.

Sample Description: Apollo sample 68815 is a polymict impact melt breccia containing a variety of lithic and mineral fragments embedded in devitrified impact melt. This sample was chipped off the top of a boulder at Station 8 during the Apollo 16 mission and had an original weight of nearly 1.8 kg. In this study, we

investigated two polished thin sections of 68815: 68815,17 and 68815,148, both containing spinel.

Methods: The thin sections of 68815 were studied using optical light microscopy (PPL, cross-polarized light, and reflected light) with a Keyence VHX-7100 Digital Microscope. Each section was then X-ray mapped for 13–14 elements using a Cameca SX100 electron probe microanalyzer (EPMA) located in the Kuiper Materials Imaging and Characterization Facility (KMICF) at the University of Arizona. We have obtained geochemical information about the phases (olivine, plagioclase, spinel, pyroxene) in the thin sections also using the EPMA. In addition, we have used ThermoScientific Helios NanoLab 660 Focused-Ion-Beam Scanning-Electron Microscope (FIB-SEM) and a Hitachi S-4800 SEM (both in KMICF) to obtain backscattered electron (BSE) images and energy dispersive X-ray spectrometry (EDS) maps of areas of interest. Using

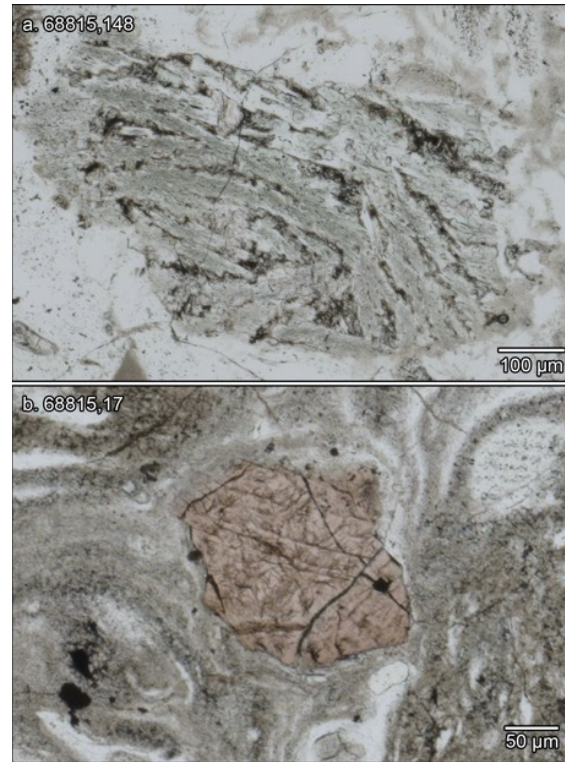


Figure 1. (a) Plane polarized light (PPL) image of a spinel-bearing clast in 68815,148. The spinel are located in the top right corner of the clast. (b) PPL image of a large spinel grain in 68815,17.

a JEOL 7900F SEM at the Astromaterials Research & Exploration Science (ARES) at NASA Johnson Space Center (JSC), we have obtained electron backscatter diffraction (EBSD) maps of the spinel-bearing portions of the thin sections. The EBSD data were collected under beam conditions of 20 kV, and \sim 90 μ A, with step sizes varying from 0.05 to 2 μ m. Following EBSD data collection, we processed the data using AZtecCrystal and MTEX, a free MATLAB toolbox.

Results: We have found clasts with subophitic textures, that consist of primarily olivine and plagioclase, with minor amounts of pink Mg-Al spinel and pyroxene (Fig. 1). These clasts are up to \sim 1 mm in length and contain spinels up to 50 μ m across. We have additionally identified pink Mg-Al spinels within the impact melt (i.e., not contained in lithic clasts) in both thin sections. In one instance, a single spinel grain is approximately 300 μ m across (Fig. 1b, 2). The spinel fragments embedded in impact melt have varying compositions, typically distinct from the compositions of spinels in the lithic clasts.

Spineland Clasts: Ten lithic clasts with similar textures and mineral compositions were identified between 68815,17 (two clasts) and ,148 (eight clasts).

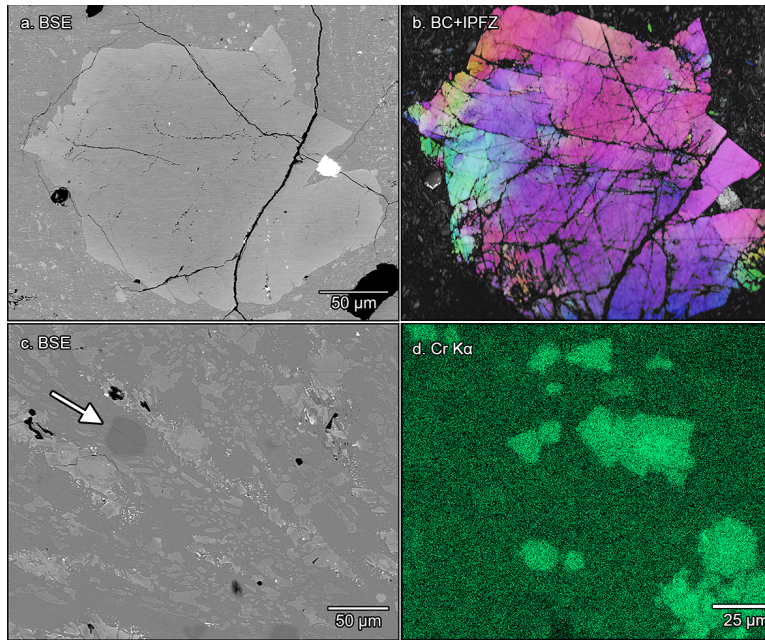


Figure 2. (a) Backscattered electron (BSE) image of large spinel grain in 68815,17 also shown in Figure 1b, with metal appearing bright white, and spinel showing Fe zoning from core to rim. (b) electron backscatter diffraction (EBSD) map of the same large spinel grain, showing the band contrast(BC) in grayscale and the inverse pole figure for the Z-axis of spinel in color (IPFZ). (c) BSE image of a subophitic textured clast in 68815,17, with spinel in dark gray (white arrow), pyroxene in bright gray, olivine light gray, and plagioclase medium gray. (d) Chromium Ka map of a spinel in a different part of the same clast as (c), exhibiting reverse zoning (enrichment inward).

These clasts fall into two groups. The first has skeletal olivine with intergranular plagioclase, with minor amounts of pyroxene and spinel (Fig. 1a, 2c, 2d). The spinel in these clasts are found amid the plagioclase. The second group have an intergranular texture of olivine and plagioclase, again with minor spinel and pyroxene. The second group may contain spinels surrounded by plagioclase, and spinels enclosed in olivine. Spinels located within both clast types range from no apparent Cr-zoning, to reverse zoning (Cr-enrichment inward; Fig. 2d), to normal zoning (Cr-enrichment outward).

In the clasts thus far investigated with EPMA, plagioclase compositions range from An# (molar $100 \times \text{Ca}/(\text{Ca}+\text{Na}+\text{K})$) 92–96. Olivine Mg# ranged from 77 to 94, while pyroxene had Mg# from 54–84. Spinel in the clasts have Cr# (molar $100 \times \text{Cr}/(\text{Cr}+\text{Al})$) 2–4 and Mg# 88–91, which is within the range of pristine and plutonic spinel troctolites [8].

Isolated Spinels: These crystals are generally euhedral to subhedral, and can exhibit reverse Cr zoning (Cr-enrichment inward) or no apparent Cr zoning. The spinels thus far investigated via EPMA have Cr# 9–14 and Mg# 65–82. The Cr# for these spinels is within the range reported by [8], but have lower Mg#.

Future Work: We will continue to process the EBSD data for these lithic and mineral clasts. We will also continue to characterize these clasts using EPMA and SEM. By thoroughly characterizing the various spinels and spinel-bearing clasts, we aim to constrain the petrogenesis of these minerals and rock fragments.

Acknowledgments: We thank NASA for the loan of these thin sections. We thank Ken Domanik and Jerry Chang for their support with data collection. Work was supported by a University of Arizona RII Core Facilities Pilot Program grant and start-up funds to JJB. We acknowledge support from NASA's Planetary Science Research program for analysis performed at JSC.

References: [1] Shearer C. K. et al. (2015) *Am. Min.* 100, 294–325. [2] Borg L. E. et al. (2020) *GCA* 290, 312–332. [3] Warren P. H. (1993) *Am. Min.* 78, 360–376. [4] Dymek R. F. et al. (1976) *LPS VII*, 2335–2378. [5] Treiman et al. (2019) *Am. Min.* 104, 370–384. [6] Pieters et al. (2011) *JGR: Plan.* 116:E00G08. [7] Prissel et al. (2016) *Icarus* 277, 319–329. [8] Prissel et al. (2016) *Am. Min.* 101, 1624–1635.